3D WERNER DECONVOLUTION OF GRAVITY DATA OF MIGORI GREENSTONE BELT, KENYA

Odek Antony[1], Githiri John[2], K'Orowe Maurice[2], Ambusso Willis[3]
[1]Chuka University, Physical Sciences Department, P.O. Box 109-60400, Chuka
[2]Jomo Kenyatta University of Agriculture and Technology, Physics Department
[3]Kenyatta University, Kenya, Physics Department

ABSTRACT

Depth imaging in gravity survey is very important in mineral prospecting. A number of techniques ranging from manual measurements of anomaly characteristic and the application of empirically derived formulae to modern automated analysis of gravity data have been developed. The automatic techniques range from standard Euler deconvolution, extended Euler deconvolution, Werner deconvolution and Analytic signal among others. The quality of interpretation depends on how well the data is constrained using other geological and geophysical information. The results can further be improved by integrating different interpretation techniques. In this study attempt has been made to interpret the depth of the gravity anomaly causative bodies in Migori Greenstone belt using 3D Werner deconvolution. Werner deconvolution technique has been widely used for rapid interpretation of magnetic data and in this study it has been extended to gravity by performing a vertical derivative to yield a pseudo magnetic field. Oasis montaj application software was then used to generate Werner solutions. Shallow gravity structures are mapped from the surface to a limiting depth of approximately 1,000 m. These structures agree well with the other interpretation techniques and known geology of the area.

Keywords: Gravity, Anomalies, Migori Greenstone belt, Deconvolution

Introduction

Convolution is a mathematical operation defining the change of shape of a waveform resulting from the passage through a filter. Its implementation involves time inversion of one of the functions and its progressive sliding past the other function, the individual terms in the convolved output being derived. Deconvolution is a process that counteracts the convolution action (Kearley et al, 2002). Werner deconvolution technique is used to analyze the depth and position of magnetic sources as well as their magnetic susceptibilities and dip along profiles (Hassan et al, 2015). It is based on the assumption that magnetic anomalies can be estimated by either thin sheet bodies or geological interfaces with infinite depth extent and arbitrary dip (Hassan et al, 2015). Attempts have been made with success to extend two dimension Werner deconvolution to three dimensions through the use of generalized Hilbert transformation (Reid et al, 1990).

A further multiple source extension of the three dimension Werner algorithm has been developed. Unlike the three dimension Euler algorithm that requires taking high order derivatives of the field, one derivative order for each source, which makes the algorithm highly dependent on data quality. The multiple source Werner deconvolution only requires first order derivatives, no matter the number of sources (Hassan et al, 2015). It has been shown by Nabighian and Hansen (2001) that extended Euler deconvolution is a generalization of Werner deconvolution and can be extended to three dimensions which is the definition of three dimensions Werner deconvolution. Depth to basement methods is designed primarily for use with total field magnetic data. However, mathematically the magnetic response is equivalent to the derivative of the gravity response, so it is possible to use depth to basement methods on the gravity profile by using either horizontal or vertical derivative of gravity as the input anomaly profile rather than total field magnetic data. With large distinct density contrasts, the extension can also be used on gravity profile to determine the position of gravity source bodies (Geosoft oasis montaj, 2007)

For the case of zero Euler index Mushayandebvu et al. (1999) obtained the following two extended Euler equations

$$(x - x_0)\frac{\partial M}{\partial x} + (z - z_0)\frac{\partial M}{\partial z} = \alpha \qquad \text{......1.1}$$

$$(x - x_0)\frac{\partial M}{\partial z} - (z - z_0)\frac{\partial M}{\partial x} = \beta \qquad \text{......1.2}$$

Where M is the gravity field, x_o, y_o and $z_o$are the unknown coordinate of the source body centre to be estimated, x,y and z are the known coordinates of the observation point of the gravity and gradients, n is the structural index, α and β are constants. These equations are equivalent to Werner deconvolution (Nabighian and Hansen, 2001). For non-zero Euler index Mushayandebvu et al equation becomes

$$(x - x_0)\frac{\partial M}{\partial x} + (z - z_0)\frac{\partial M}{\partial z} + nM = 0 \qquad \text{......1.3}$$

$$(x - x_0)\frac{\partial M}{\partial z} - (z - z_0)\frac{\partial M}{\partial x} + n\mathrm{H}(M) = 0 \qquad \text{......1.4}$$

Where H denotes Hilberts transform. Using Cauchy-Riemann equations (Nabighian, 1972) the equations reduces to

$$\frac{\partial M}{\partial x} = -\frac{\partial}{\partial z} H(M) \quad \text{..........1.5}$$

$$\frac{\partial M}{\partial z} = \frac{\partial}{\partial x} H(M) \quad \text{..........1.6}$$

And hence equation 1.4 becomes

$$(x - x_0)\frac{\partial}{\partial x} H(M) + (z - z_0)\frac{\partial}{\partial z} H(M) + nH(M) = 0 \quad \text{..........1.7}$$

This shows that equation 1.4 is equivalent to the assumption that if a two dimensional potential field is homogeneous with Euler index n, then so is its Hilbert transform. The general case can be written in the form

$$(x - x_0)\frac{\partial M}{\partial x} + (z - z_0)\frac{\partial M}{\partial z} + nM = \alpha \quad \text{..........1.8}$$

$$(x - x_0)\frac{\partial}{\partial x} H(M) + (z - z_0)\frac{\partial}{\partial z} H(M) + nH(M) = \beta \quad \text{..........1.9}$$

Where α and β will generally vanish unless n=0. Equations 1.8 and 1.9 gives a unification and a generalization of Euler and Werner deconvolution in the 2D case and suggests that the algorithm might be extended to three dimensions, thereby providing both an extension of Werner deconvolution to the three dimensions case and a generalization of the Euler equations (Nabighian and Hansen, 2001). They also showed that assuming M satisfies Laplace's equation and also satisfies the generalised Euler equation with index n and define the three dimension Hilberts transforms as in Nabighian (1984) then two more equations are obtained which is compact form can be written as:

$$(x - x_0)\frac{\partial}{\partial x} H(M) + (y - y_0)\frac{\partial}{\partial y} H(M) + (z - z_0)\frac{\partial}{\partial z} H(M) + nH(M) = \beta \quad \text{..........1.10}$$

This provides a generalization of both Euler deconvolution and Werner deconvolution in three dimensions. The new algorithm helps stabilize the Euler algorithm by providing at each point three equations for each measured field rather than one. Gravity sources are easily treated by performing a vertical derivative to yield a pseudo magnetic field. The idea is to solve the equation as a least square system followed by extraction of the source locations from the coefficients.

Methodology

Data acquisition

Ground gravity data was collected from 425 stations established over an area of approximately 200 km^2 bounded by the latitudes 34˚15'E -34˚40'E and longitudes 0˚55'S – 1˚12'S in Migori, Mac alder and Kehancha areas (Figure 2.1), with station and profile spacing of approximately 300 m and 1 km respectively. Gravity measurements were taken using Gravity meter prospect W45.Variations in the earth's gravity which did not result from the differences in density of the underlying rocks were corrected from the ground survey data.This includes instrumental drift, free air variation, Bourguer slab, latitude and terrain effects.

The theoretical value of gravity ($g_{\emptyset}$) at given latitude ($\emptyset$) was calculated using gravity formula (World geodetic system, 1984)

$$g_{\emptyset} = 9.7803267714\ 1 + 0.00193185138639 sin^2\emptyset / \sqrt{1 - 0.00669437999013 sin^2\emptyset} ms^{-2}$$ …………………..…2.1

and it was subtracted from or added to the measured value to isolate latitude effect. As one moves away from the center of the earth, gravity decreases, the rate of decrease can be deduced by assuming spherical earth. From

$$g = GM/r^2$$ ……………………………………………………………………………………………….………2.2

$$\delta g/\delta r = -2\,g/r = -0.3086\Delta h$$ ……………………………………………………………….…………………………….2.3

Where g is gravity, G is the universal gravity constant, r is the distance from Centre of the earth, M is the mass of the earth and h is the altitude. For the sites which were above the reference point, free air correction was added to the observed gravity value. For the sites which were below the reference point, free air correction was subtracted from the observed gravity value. Bouguer correction ($g = 2\pi G\rho\Delta hg$) where ρ is the average crustal density, was done to remove the effect of attraction of a slab of rock present between the observation point and the datum. Terrain correction was also conducted to remove the effect of a hill or a valley at the vicinity of a station, which ultimately reduces the gravity value.

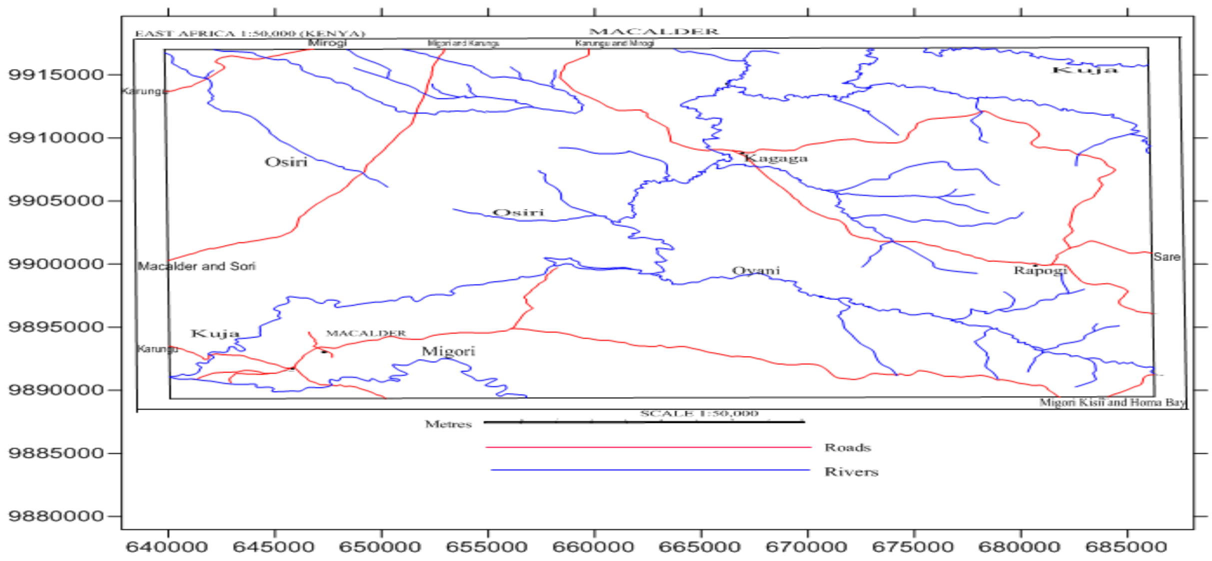

Figure 2.1: Digitized map of Mac alder showing drainage features

Data Analysis

Shaded colour contour map of the complete bourguer anomaly (Figure 2.2) was drawn using Geosoft Oasis Montaj program. The localized gravity anomalies caused by rocks are superimposed on the regional trends. The data was then subjected to low pass filtering to remove the regional trends (Figure 2.3). The same was used to generate Werner solutions with the vertical derivative of gravity used as the input anomaly profile. The inclination was set to 90^0 while declination set to 0^0. Field strength of 10 which give the best conversion of susceptibilities to densities (Geosoft oasis montaj, 2007) was used. The minimum and maximum depths were set at 0 m and 4,000 m respectively, any solution below the minimum depth or above the maximum depth is discarded. Profiles for both contacts and dikes are displayed with their corresponding spray of solutions (Figure 2.4). Given the low noise level in the data, a low residual cut-off value of 2 was used. It sets the amplitude threshold for the anomalies and can also be used to eliminate noise in the data.

The colour shaded contour map delineates a high gravity anomaly trending ESE-WNW, Werner solution result was latter interpreted based on the concentration of solutions, the higher the concentration of solution, the higher the probability of finding the causative body at that depth. Further attempts were made to contour the obtained Werner depths (Figure 2.5). Shallow causative body depths of between 500 m to 1,500 m are obtained.

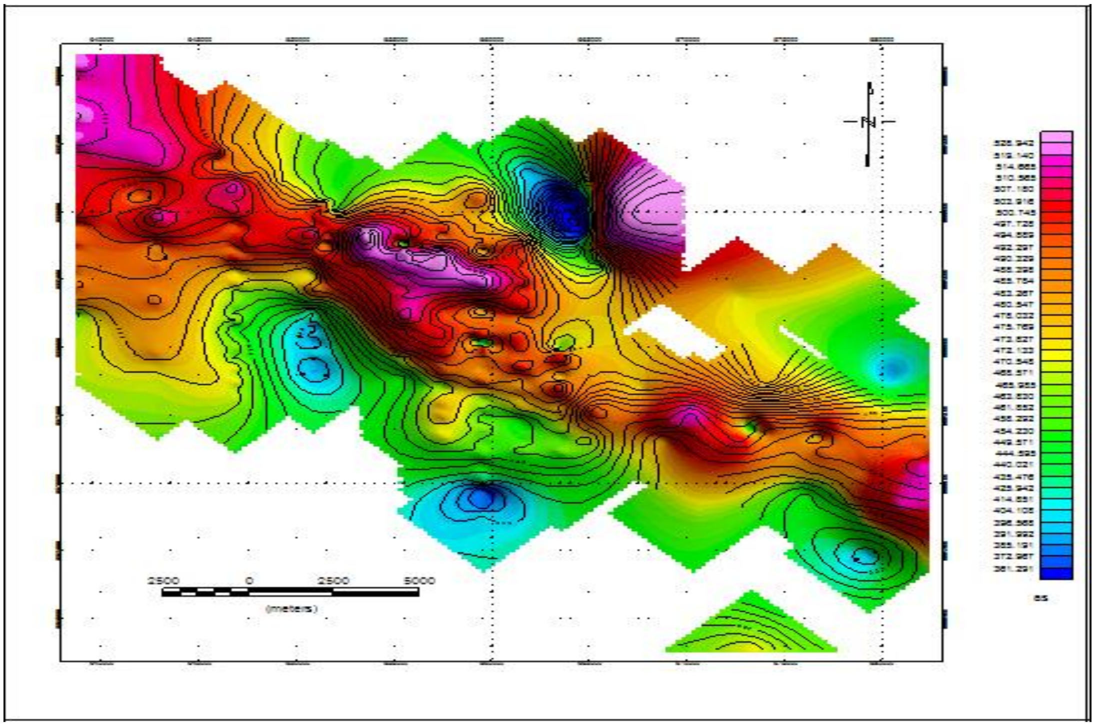

Figure 2.2: Shaded colour relief of the complete Bouguer anomaly

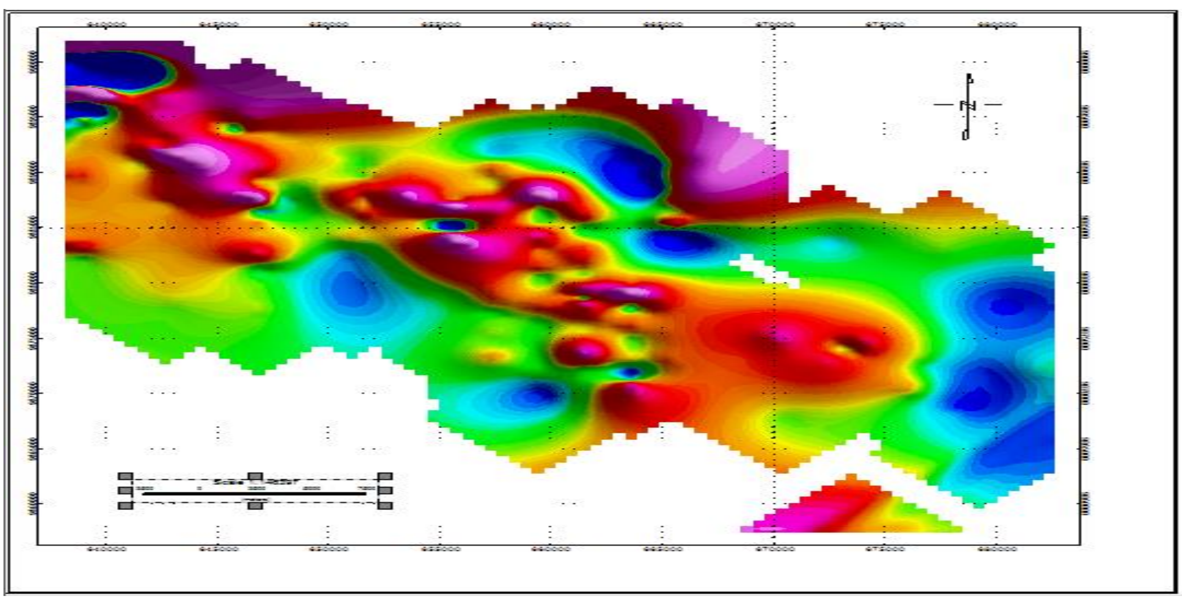

Figure 2.3: Shaded colour contour map of the low pass filtered data of Migori Greenstone belt

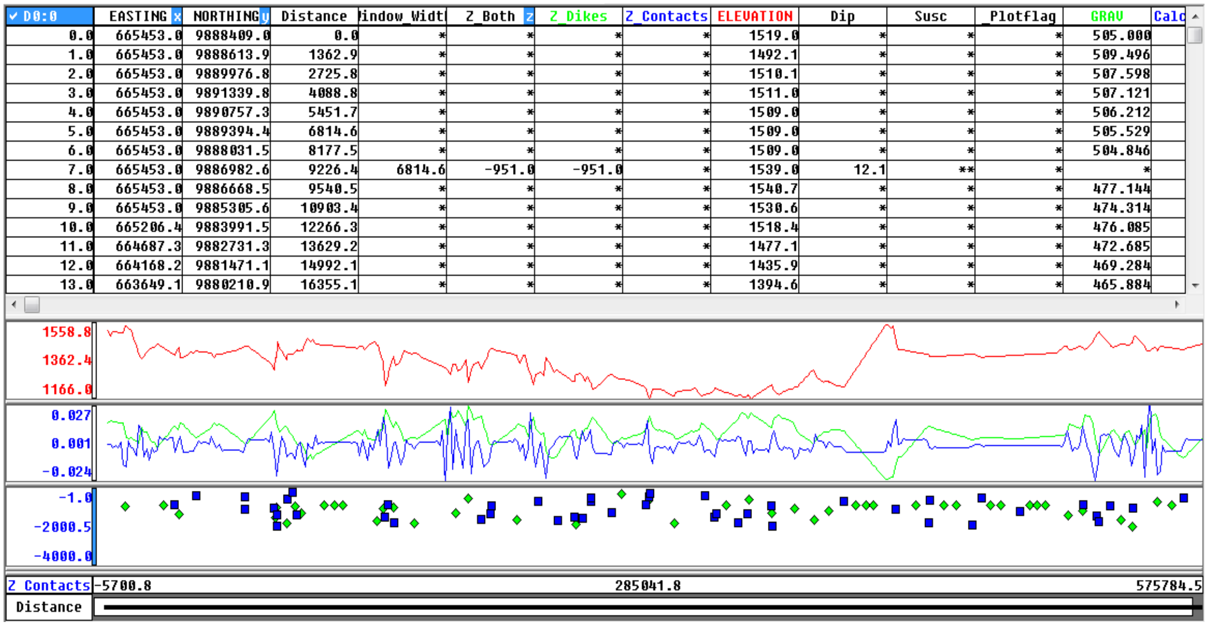

D0:0	EASTING	NORTHING	Distance	Window_Widt	Z_Both	Z_Dikes	Z_Contacts	ELEVATION	Dip	Susc	_Plotflag	GRAV	Calc
0.0	665453.0	9888409.0	0.0	*	*	*	*	1519.0	*	*	*	505.000	
1.0	665453.0	9888613.9	1362.9	*	*	*	*	1492.1	*	*	*	509.496	
2.0	665453.0	9889976.8	2725.8	*	*	*	*	1510.1	*	*	*	507.598	
3.0	665453.0	9891339.8	4088.8	*	*	*	*	1511.0	*	*	*	507.121	
4.0	665453.0	9890757.3	5451.7	*	*	*	*	1509.0	*	*	*	506.212	
5.0	665453.0	9889394.4	6814.6	*	*	*	*	1509.0	*	*	*	505.529	
6.0	665453.0	9888031.5	8177.5	*	*	*	*	1509.0	*	*	*	504.846	
7.0	665453.0	9886982.6	9226.4	6814.6	-951.0	-951.0	*	1539.0	12.1	**	*	*	
8.0	665453.0	9886668.5	9540.5	*	*	*	*	1540.7	*	*	*	477.144	
9.0	665453.0	9885305.6	10903.4	*	*	*	*	1530.6	*	*	*	474.314	
10.0	665206.4	9883991.5	12266.3	*	*	*	*	1518.4	*	*	*	476.085	
11.0	664687.3	9882731.3	13629.2	*	*	*	*	1477.1	*	*	*	472.685	
12.0	664168.2	9881471.1	14992.1	*	*	*	*	1435.9	*	*	*	469.284	
13.0	663649.1	9880210.9	16355.1	*	*	*	*	1394.6	*	*	*	465.884	

Figure 2.4: Werner solutions for both dykes and contacts

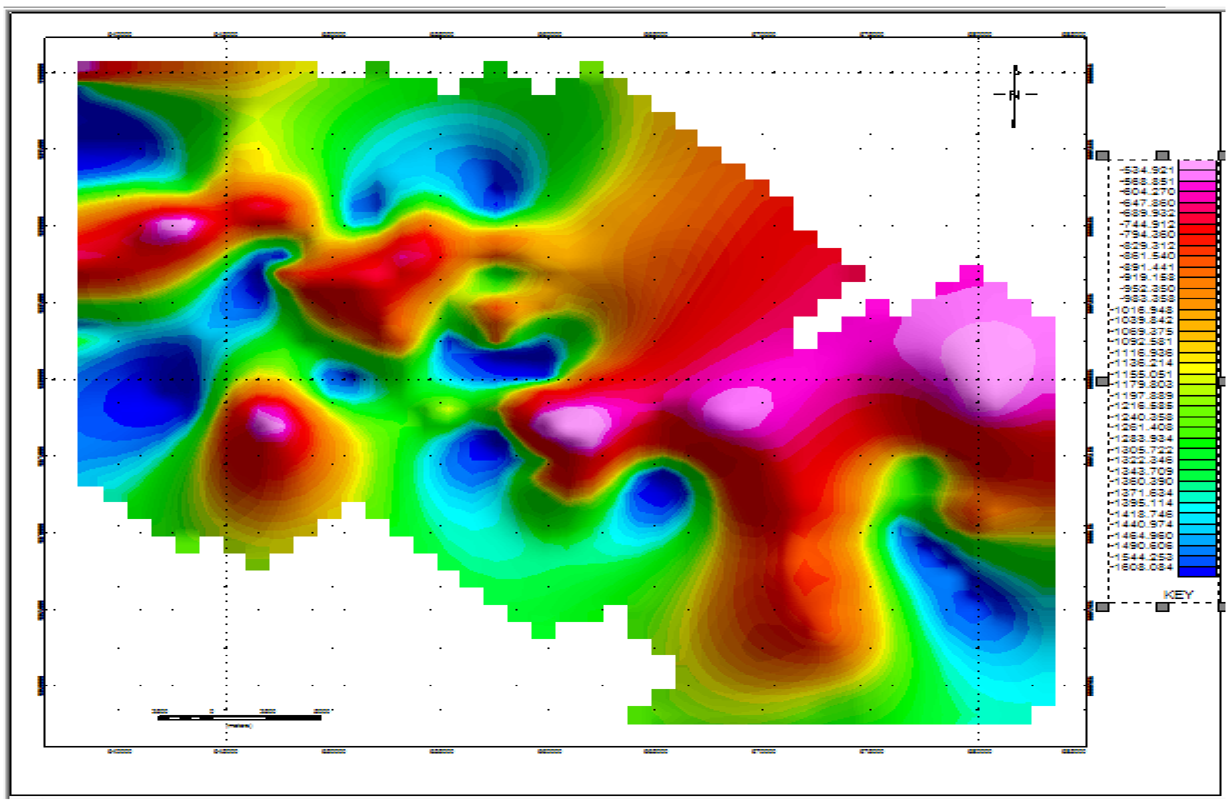

Figure 2.5: Shaded colour contour of Werner depths

Two profiles AA and BB were further taken across the anomaly at two different points (Figure2.6). Gravity amplitudes of 520 mgal and 500 mgalare obtained across the anomalies along profiles AA and BB respectively. The profiles were further subjected to Werner deconvolution in order to obtain the possible depth of the causative bodies along these profiles (Figure 2.7 and Figure 2.8). Anomaly causative bodies were mapped at shallow depths of up to 1,500 m from the ground surface for profile AA and up to about 1,000 m for profile BB.

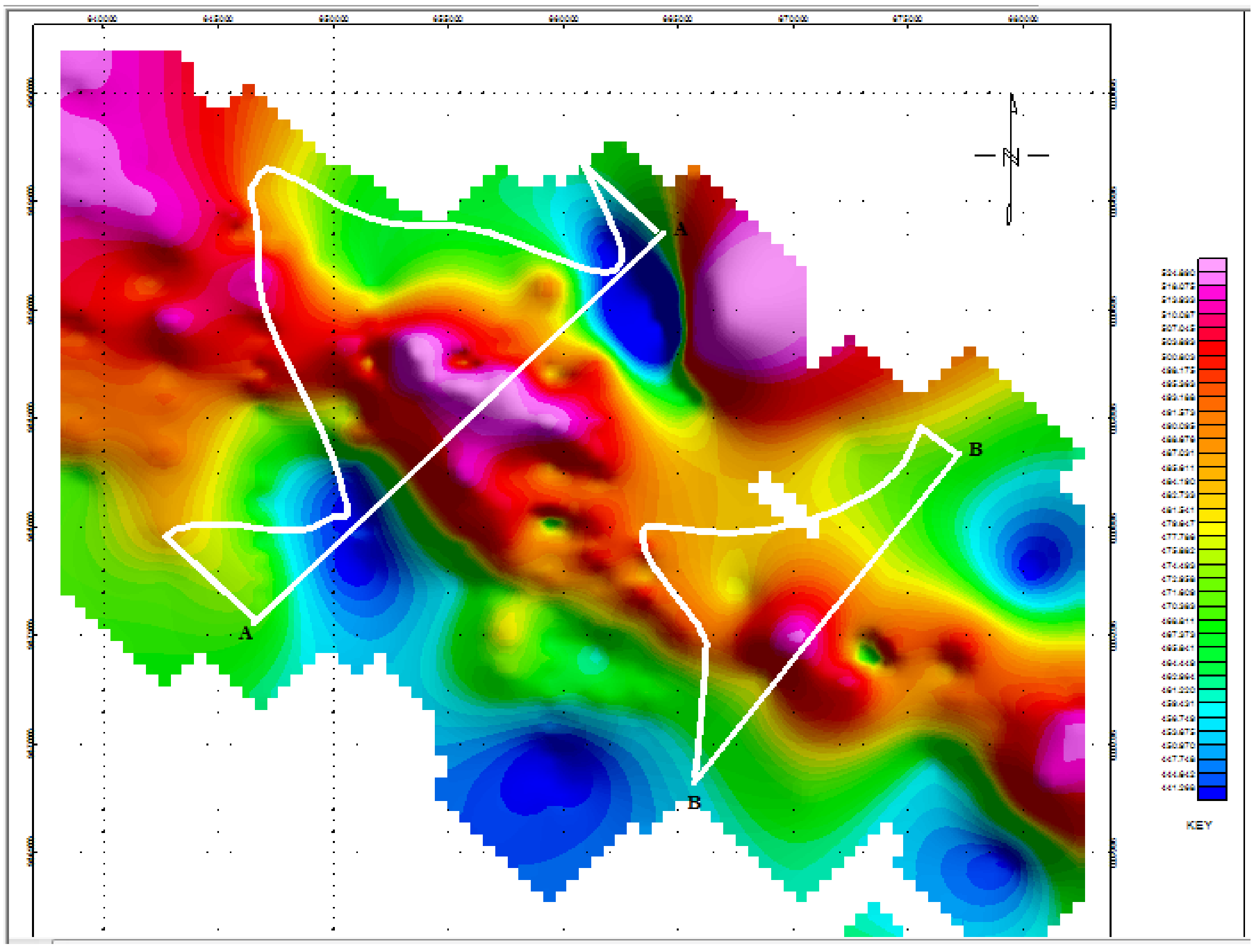

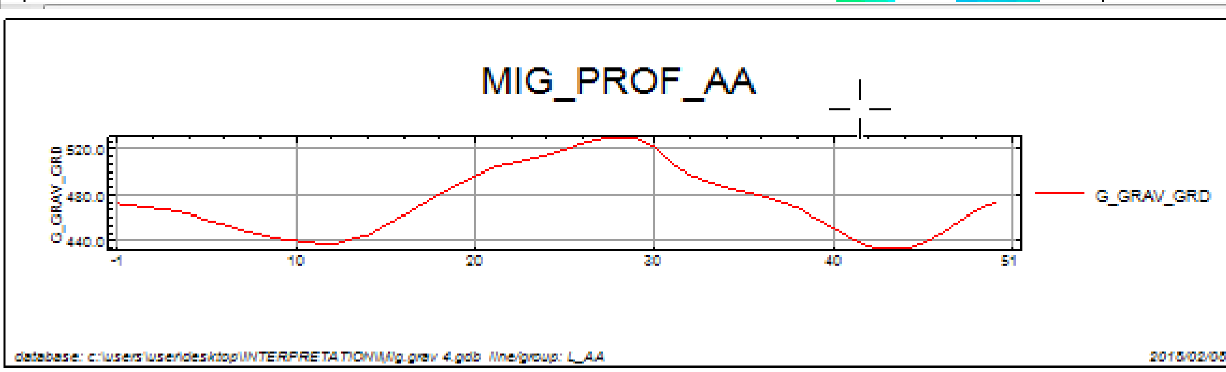

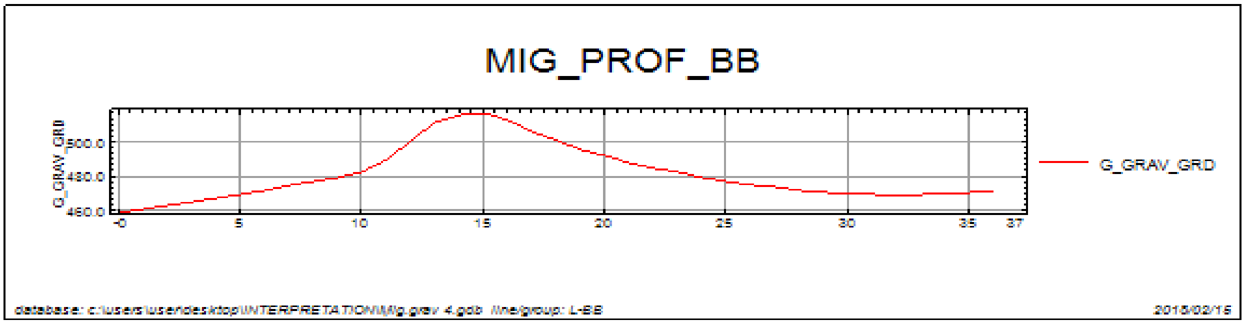

Figure 2.6: Profiles AA and BB

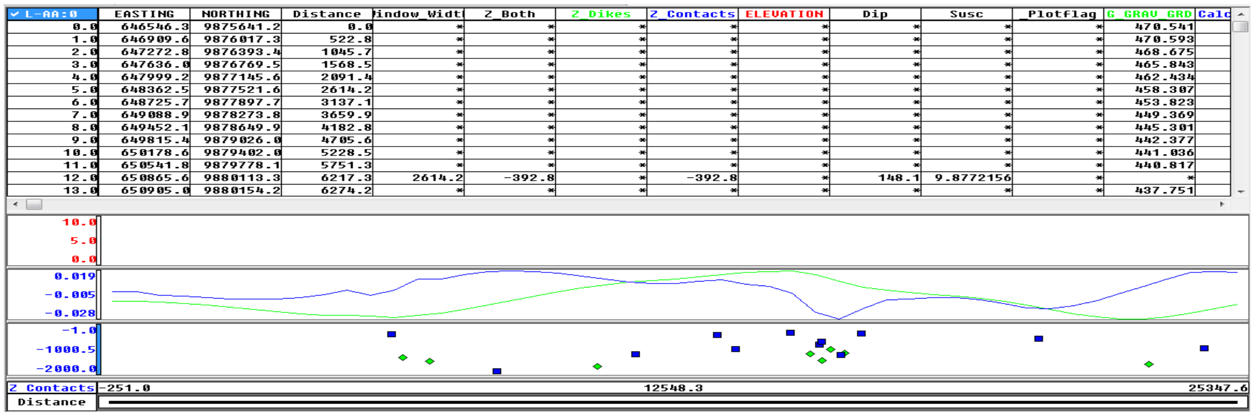

L-AA:0	EASTING	NORTHING	Distance	Window_Widt	Z_Both	Z_Dikes	Z_Contacts	ELEVATION	Dip	Susc	_Plotflag	G_GRAV_GRD	Calc
0.0	646546.3	9875641.2	0.0	*	*	*	*	*	*	*	*	470.541	
1.0	646909.6	9876017.3	522.8	*	*	*	*	*	*	*	*	470.593	
2.0	647272.8	9876393.4	1045.7	*	*	*	*	*	*	*	*	468.675	
3.0	647636.0	9876769.5	1568.5	*	*	*	*	*	*	*	*	465.843	
4.0	647999.2	9877145.6	2091.4	*	*	*	*	*	*	*	*	462.434	
5.0	648362.5	9877521.6	2614.2	*	*	*	*	*	*	*	*	458.307	
6.0	648725.7	9877897.7	3137.1	*	*	*	*	*	*	*	*	453.823	
7.0	649088.9	9878273.8	3659.9	*	*	*	*	*	*	*	*	449.369	
8.0	649452.1	9878649.9	4182.8	*	*	*	*	*	*	*	*	445.301	
9.0	649815.4	9879026.0	4705.6	*	*	*	*	*	*	*	*	442.377	
10.0	650178.6	9879402.0	5228.5	*	*	*	*	*	*	*	*	441.036	
11.0	650541.8	9879778.1	5751.3	*	*	*	*	*	*	*	*	440.817	
12.0	650865.6	9880113.3	6217.3	2614.2	-392.8	*	-392.8	*	148.1	9.8772156	*	*	
13.0	650905.0	9880154.2	6274.2	*	*	*	*	*	*	*	*	437.751	

Figure 2.7: Werner solutions along profile AA

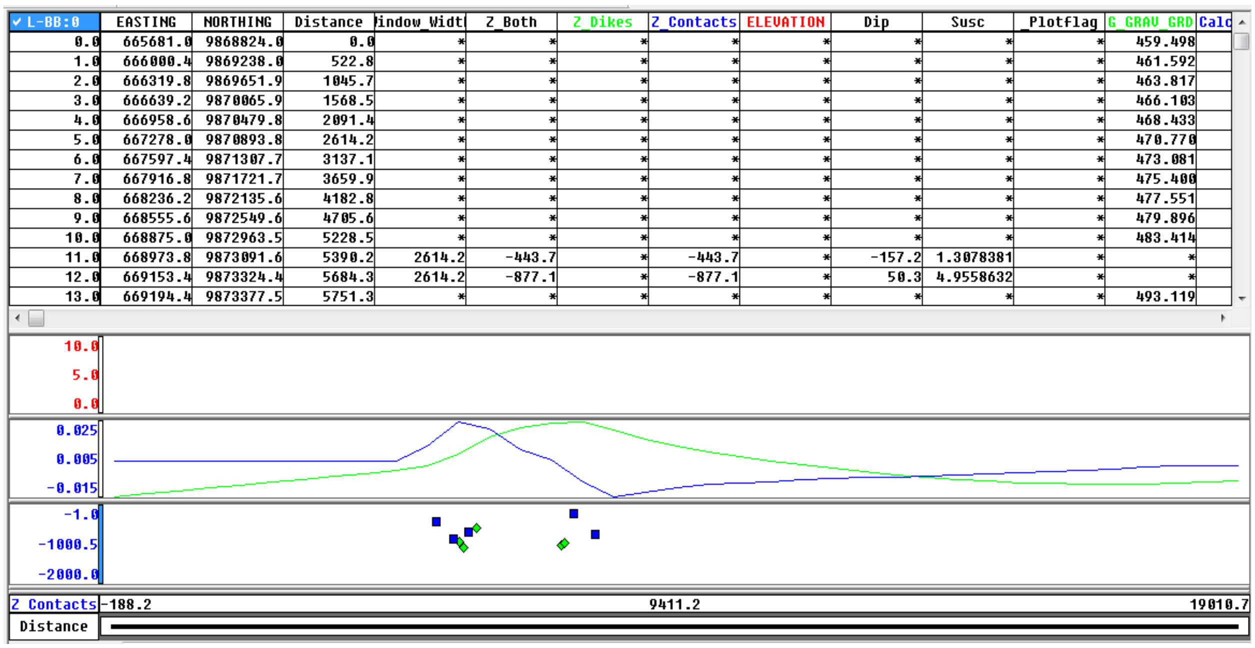

L-BB:0	EASTING	NORTHING	Distance	Window_Widt	Z_Both	Z_Dikes	Z_Contacts	ELEVATION	Dip	Susc	_Plotflag	G_GRAV_GRD	Calc
0.0	665681.0	9868824.0	0.0	*	*	*	*	*	*	*	*	459.498	
1.0	666000.4	9869238.0	522.8	*	*	*	*	*	*	*	*	461.592	
2.0	666319.8	9869651.9	1045.7	*	*	*	*	*	*	*	*	463.817	
3.0	666639.2	9870065.9	1568.5	*	*	*	*	*	*	*	*	466.103	
4.0	666958.6	9870479.8	2091.4	*	*	*	*	*	*	*	*	468.433	
5.0	667278.0	9870893.8	2614.2	*	*	*	*	*	*	*	*	470.770	
6.0	667597.4	9871307.7	3137.1	*	*	*	*	*	*	*	*	473.081	
7.0	667916.8	9871721.7	3659.9	*	*	*	*	*	*	*	*	475.400	
8.0	668236.2	9872135.6	4182.8	*	*	*	*	*	*	*	*	477.551	
9.0	668555.6	9872549.6	4705.6	*	*	*	*	*	*	*	*	479.896	
10.0	668875.0	9872963.5	5228.5	*	*	*	*	*	*	*	*	483.414	
11.0	668973.8	9873091.6	5390.2	2614.2	-443.7	*	-443.7	*	-157.2	1.3078381	*	*	
12.0	669153.4	9873324.4	5684.3	2614.2	-877.1	*	-877.1	*	50.3	4.9558632	*	*	
13.0	669194.4	9873377.5	5751.3	*	*	*	*	*	*	*	*	493.119	

Figure 2.8: Werner solutions along profile BB

Discussions and Conclusion

The gravity data of Migori greenstone belt delineates high gravity anomalies of amplitude of up to 525 mgal. The structures trends ESE-WNW from Kenya-Tanzania border through Kehancha, Masaba, Nyanchabo, Migori, Mukuro, Masara, all through to Macalder. These regions have witnessed a lot of artisan mining using opencast method (Ichangi, 1993). The Werner technique maps these dense structures from the ground surface to depth of about 1,500 m. The gravity highs are sandwiched by the high gravity gradients that are interpreted as fault lines. The causative structures are associated with granitic intrusive characterised by banded iron formations that also act as a host for other minerals.These structures agree well with the other interpretation techniques and known geology of the area (Shackleton, 1946).

References

Geosoft (Oasis Montaj) *program, Geosoft mapping and Application system*. Inc. Suit 500, Richmond St. West Toronto, ON Canada N5S1V6. User's Manual 2007.

Ichangi D.W. (1993).Lithostratigraphic setting of mineralization in the Migori segment of the Nyanza Greenstone Belt, Kenya. *In: Proceedings of the fifth conference of the geology of Kenya*. Nairobi, Kenya.

Kearey P., Michael B., Ian H. (2002). *An Introduction to Geophysical Exploration*. 3rd edition. London: Blackwell Scientific publications.

Mushayandebvu, M.F., van Driel, P., Reid, A.B. and Fairhead, J.D., 1999, Magneticimaging using extended Euler deconvolution: Presented at the 69th Ann. Internat. Mtg., Soc. Expl. Geophys.

Nabighian, M.N. and Hansen R.O., 2001. Unification of Euler and Werner deconvolution in three dimensions via the generalized Hilbert transform. Society of Exploration Geophysicists, 1805-1810.

Nabighian, M.N., 1984, Toward a three-dimensional automatic interpretation of potential field data via generalized Hilbert transforms: Fundamental relations: Geophysics, 49,780-786.

Nabighian, M.N., 1972, The analytic signal of two-dimensional magnetic bodies with polygonal cross-section: Its properties and use for automated interpretation: Geophysics,37, 507-517.

Reid, A. B., Allsop, J. M., Granser, H., Millett, A. J., and Somerton, I. W. [1990] Magnetic interpretation in three dimensions using Euler deconvolution. Geophysics. **55**, 80–91.

Shackle ton R.M. (1946). Geology of Migori Gold belt and adjoining areas. *Geological survey of Kenya*, Mining and Geological Department Kenya, Rept. **10**: 60.

World geodetic system, (1984). Ellipsoidal gravity formula. *Department of defence and World geodetic systems*, Washington DC.